Exact occupation probabilities for intermittent transport and application to image correlation spectroscopy

Coppola, S.; Caracciolo, G.; Schmidt, T.

Exact occupation probabilities for intermittent transport and application to image correlation spectroscopy

2014 New J. Phys. 16 113057

(http://iopscience.iop.org/1367-2630/16/11/113057)

New Journal of Physics
The open access journal at the forefront of physics
Deutsche Physikalische Gesellschaft DPG | IOP Institute of Physics

Exact occupation probabilities for intermittent transport and application to image correlation spectroscopy

S Coppola[1], G Caracciolo[2,3] and T Schmidt[4]

[1] Deparment of Anatomy, Histology, Forensic Medicine and Orthopedics, 'Sapienza' University of Rome, Piazzale A. Moro 5, I-00185, Rome, Italy
[2] Department of Molecular Medicine, 'Sapienza' University of Rome, Piazzale A. Moro 5, I-00185, Rome, Italy
[3] Center for Life Nano Science @Sapienza, Istituto Italiano di Tecnologia, viale Regina Elena 291, I-00161 Rome, Italy
[4] Physics of Life Processes, Huygens-Kamerlingh Onnes Laboratory, Leiden University, Niels Bohrweg 2-2333 CA Leiden, The Netherlands
E-mail: schmidt@physics.leidenuniv.nl

Received 17 July 2014, revised 19 September 2014
Accepted for publication 8 October 2014
Published 24 November 2014
New Journal of Physics **16** (2014) 113057
doi:10.1088/1367-2630/16/11/113057

Abstract

Intermittent transport is frequently observed in nature and has been proven to accelerate search processes at both the macroscopic (e.g., animals looking for food) and microscopic scale (e.g., protein-DNA interactions). In living cells, active transport of membrane proteins (e.g., membrane receptors) or intracellular vesicles (organelles) has been extensively studied as an example of intermittent behavior. The intermittent stochastic process is commonly analyzed in terms of first-passage probabilities. Here we derive exact occupation probabilities of intermittent active transport, making such analysis available for image correlation spectroscopy techniques. The power of this new theoretical framework is demonstrated on intracellular trafficking of lipid/DNA nanoparticles in living cells for which we were allowed to quantify switching time scales.

Keywords: intermittent transport, intracellular trafficking, active transport, lipid/DNA nanoparticles

1. Introduction

Intermittent mobility and transport, the stop and go movement, is a ubiquitous process that occurs during cargo transport in inhomogeneous media, shuttling proteins in a cell, according to human traffic patterns [1, 2]. It has been argued that in some circumstances, intermittent movement has a distinct advantage in target finding processes that span, on macroscopic scales, from animals and bacteria looking for food [3] to, on the microscopic scale, the transport of vesicles to specific sites [4, 5]. A particular cellular process that lies at the heart of neurotransmitter transport in axons and the gene delivery by natural and synthetic viruses is that of DNA-filled vesicle transport. This transport is characterized by a frequent switching between a passive diffusive mode and an active transport driven by molecular motors [6]. Various motor proteins such as kinesins, dyneins, or myosins are able to convert the chemical fuel provided by adenosine triphosphate (ATP) into mechanical work by interacting with the semiflexible oriented filaments (mainly F-actin and microtubules) of the cytoskeleton [7]. Because many molecules or larger cellular organelles such as vesicles, lysosomes, or mitochondria can randomly bind and unbind to motors, the overall transport in the cell is faithfully described by alternating (intermittent) phases of standard diffusive transport and phases of active directed transport powered by motor proteins [4, 6].

Various experimental strategies have been developed that allow one to study the transport of vesicles in live cells at high spatial and temporal resolution. These include the direct visualization by single particle tracking (SPT) [6, 8–11] and a variety of image correlation spectroscopy (ICS) techniques [12–15]. Typically, data obtained from these techniques are analyzed in terms of mean squared displacements [16–18] that result in mean diffusion constants and mean transport velocities for the objects. Due to the averaging procedure, information about multiple independent populations and typical switching times is lost, despite the exquisite resolution the experimental techniques generate.

Here we derive the theoretical framework that allows one to use the full information density on squared-displacement distribution functions that are contained in tracking and correlation data. We obtained the exact occupation probability distribution for particles undergoing an n-state intermittent behavior between diffusive and active transport modes in a d-dimensional space. Our result can be applied to all ICS techniques, such as spatio-temporal ICS (STICS) [19] (or its k- and ν-space versions [20, 21]) and to particle ICS (PICS) [22] that is based on SPT containing super-resolution information.

The theoretical framework is subsequently applied to and validated by analysis of the intermittent transport properties of cationic-lipid/DNA nanoparticles in live cells by means of PICS. We found that a major fraction ($\langle\alpha\rangle = 0.63 \pm 0.05$) of nanoparticles experienced transitions between active and passive transport, while a minor fraction was locally trapped in subcellular crowded regions (e.g., the perinuclear region). Further, we determined average values of diffusion coefficients ($\langle D\rangle = (7.6 \pm 2.0)10^{-4}\ \mu\mathrm{m}^2\,\mathrm{s}^{-1}$) and velocities ($\langle v\rangle = 34 \pm 6\ \mathrm{nm\,s}^{-1}$) that corroborate our previous results by SPT and STICS [15, 23, 24]. In addition, the method allowed us to investigate the time scales of the intermittent behavior, i.e., the average time scales T_1 and T_2 of diffusion and active transport, respectively, which define the corresponding average steady-state probabilities $\langle p_1^{SS}\rangle = \langle T_1/(T_1 + T_2)\rangle = 0.77 \pm 0.06$ and $\langle p_2^{SS}\rangle = \langle T_2/(T_1 + T_2)\rangle = 0.23 \pm 0.06$.

We have previously demonstrated that a lower transfection efficiency is related to lysosomal degradation, which, in turn, is enhanced by microtubule-mediated active transport [23]. An active transport with a large time scale might therefore increase degradation by lysosomal compartments, lowering the overall efficiency of the nanoparticles. This method can therefore highlight the correlation between switching time scales and transfection efficiencies of non-viral nanoparticles made of different lipid formulations.

2. Displacement distributions in intermittent transport

Our theoretical description was inspired by Shlesinger & Klafter [16] who derived a probabilistic description of diffusive transport that is interlaced with random trapping events. For intermittent behavior between n mobility states (e.g., diffusion characterized by diffusion constant D_i, transport characterized by velocity v_i, trapped $D_i = v_i = 0$) in a d-dimensional space, the occupation probability for a particle in mobility state i to be at position $\vec{r}$ after a (relative) time t is given by:

$$\phi_i(\vec{r}, t) = p_i\left(\vec{r} \,\middle|\, t\right)\phi_i(t) \qquad i = 1, 2, 3 \ldots n \tag{1}$$

where $p_i(\vec{r} \mid t)$ is the probability to be at $\vec{r}$ given that the time spent in phase i is t. The subscript i indicates only that the probability densities refer to state i and it is not a random variable in the distribution, nor does it indicate if the probability is conditional on being in state i. $\phi_i(t)$ is the probability density that the transport process lasts for a time t before the particle switches to a state $j \neq i$ with different transport characteristics (note that $\int_{\mathbb{R}^d} \phi_i(\vec{r}, t)d\vec{r} = \phi_i(t)$, since $\int_{\mathbb{R}^d} p_i(\vec{r} \mid t)d\vec{r} = 1$, and $\int_0^\infty \phi_i(t)dt = 1$).

The occupation probability $P(\vec{r}, t)$ of being at position $\vec{r}$ at time t is more complicated. It can be built from a memoryless Markovian scheme. The particle can reach position $\vec{r}$ at time t while being in state i at position $\vec{r} - \vec{r'}$ at an earlier time $t - \tau$. The state i might be the result of a transition from state $j \neq i$ in $\vec{r'} - \vec{r''}$ at an even earlier time $\tau - \tau'$. Therefore, its general form is:

$$\begin{aligned} P\left(\vec{r}, t\right) = &\int_{\mathbb{R}^d} \int_0^t d\vec{r'}\, d\tau \;\; Q\left(\vec{r} - \vec{r'}, t - \tau\right) \\ &\times \sum_{i=1,\, j=1}^{n} \left(\frac{1}{n-1} A_{ij}\left(\vec{r'}, \tau\right) + S_{ij}\left(\vec{r'}, \tau\right) \right) \end{aligned} \tag{2}$$

where $Q(\vec{r} - \vec{r'}, t - \tau)$ satisfies the Markovian chain Green's function equation and it is the propagator for this stochastic process [16]. $A_{ij}(\vec{r'}, \tau)$ and $S_{ij}(\vec{r'}, \tau)$ are the asymmetric and symmetric transition probabilities from state i to state j, respectively, as given by:

$$\begin{aligned} A_{ij}\left(\vec{r'}, \tau\right) = &\left(1 - \delta_{ij}\right) \int_{\mathbb{R}^d} \int_0^\tau d\vec{r''}\, d\tau'\, p_i\left(\vec{r'} - \vec{r''} \,\middle|\, \tau - \tau'\right) \\ &\times \left(\int_{\tau - \tau'}^\infty \phi_i(x)dx \right) p_j\left(\vec{r''} \,\middle|\, \tau'\right) \phi_j(\tau') p_j^{SS} \end{aligned} \tag{3}$$

$$S_{ij}\left(\vec{r'}, \tau\right) = \delta_{ij}\, p_i\left(\vec{r'} \,\middle|\, \tau\right) \int_\tau^\infty \phi_i(x)dx\, p_i^{SS} \tag{4}$$

where p_i^{SS} is the steady-state probability of state i.

We seek the solution of (2), which is most easily obtained in Fourier–Laplace space leading to the following *master equation*:

$$
\begin{aligned}
P\left(\vec{k}, s\right) &= Q\left(\vec{k}, s\right) \sum_{i=1,\, j=1}^{n} \left(\frac{1}{n-1} A_{ij}\left(\vec{k}, s\right) + S_{ij}\left(\vec{k}, s\right) \right) \\
A_{ij}\left(\vec{k}, s\right) &= \left(1 - \delta_{ij}\right) \mathcal{L} \left\{ p_i\left(\vec{k} \,\middle|\, t\right) \int_t^{\infty} \phi_i(x) dx \right\} \phi_j\left(\vec{k}, s\right) p_j^{SS} \\
S_{ij}\left(\vec{k}, s\right) &= \delta_{ij}\, \mathcal{L} \left\{ p_i\left(\vec{k} \,\middle|\, t\right) \int_t^{\infty} \phi_i(x) dx \right\} p_i^{SS} \\
Q\left(\vec{k}, s\right) &= \left(1 - \prod_{i}^{n} \phi_i\left(\vec{k}, s\right) \right)^{-1}
\end{aligned}
\tag{5}
$$

where $\phi_i(\vec{k}, s)$ is the Fourier–Laplace transform of (1) (i.e., $\phi_i(\vec{k}, s) = \mathcal{L}\left\{p_i(\vec{k} \mid t)\, \phi_i(t)\right\}$).

Given a probability distribution, which describes a particular mobility state $p_i(\vec{r} \mid t)$ and a distribution for switching times between states $\phi_i(t)$, the final probability distribution $P(\vec{k}, s)$ is obtained.

For the sake of concreteness, in what follows, we simply assume state i, i.e., $p_i(\vec{r} \mid t)$, describes a biased diffusion mobility characterized by a diffusion constant D_i and velocity v_i, i.e., $p_i(\vec{r} \mid t) = (4\pi D_i t)^{-d/2} \exp\left(-|\vec{r} - \vec{v}_i t|^2 / 4 D_i t\right)$, and the transition distribution $\phi_i(t)$ to be exponential, i.e., $\phi_i(t) = \lambda_i \exp(-\lambda_i t) = 1/T_i \exp(-t/T_i)$. Under these assumptions, (5) gives:

$$
\begin{aligned}
P\left(\vec{k}, s\right) = &\left(1 - \prod_{i}^{n} \phi_i\left(\vec{k}, s\right) \right)^{-1} \\
&\times \sum_{i=1,\, j=1}^{n} \left(\frac{1 - \delta_{ij}}{n-1} \phi_i\left(\vec{k}, s\right) \phi_j\left(\vec{k}, s\right) \frac{p_j^{SS}}{\lambda_i} + \delta_{ij} \phi_i\left(\vec{k}, s\right) \frac{p_i^{SS}}{\lambda_i} \right)
\end{aligned}
\tag{6}
$$

We note that $P(\vec{r}, t)$ is properly normalized (i.e., $\int_{\mathbb{R}^d} P(\vec{r}, t) d\vec{r} = 1$ or, in Fourier-Laplace space, $P(\vec{0}, s) = 1/s$ since $\phi_i(\vec{0}, s) = \lambda_i/(s + \lambda_i)$, $\sum_{i=1}^{n} p_i^{SS} = 1$ and $p_i^{SS} = \lambda_i^{-1} / (\sum_{i=1}^{n} \lambda_i^{-1})$).

For the diffusion with trapping case in 2-dimensional space ($d = 2$, $n = 2$, $D_1 = v_1 = 0$, $D_2 = D$, and $v_2 = 0$), (6) leads to:

$$
P\left(\vec{k}, s\right) = \frac{1}{\lambda_1 + \lambda_2} \cdot \frac{s\left(\lambda_1 + \lambda_2\right) + k^2 D \lambda_2 + \left(\lambda_1 + \lambda_2\right)^2}{\left(s + \lambda_1\right)\left(s + \lambda_2 + k^2 D\right) - \lambda_1 \lambda_2}
\tag{7}
$$

which is equivalent to the expression found by Shlesinger & Klafter [16].

The general solution we found in (6) has further interesting properties that are noteworthy to mention: (i) (6) is also valid for the limiting case $n = 1$ (i.e., no intermittent behavior but only one biased diffusion distribution, $P(\vec{k}, s) = \mathcal{L}\left\{\mathcal{F}\left\{p_1(\vec{r} \mid t)\right\}\right\}$); (ii) for any n the inverse Laplace transform $P(\vec{k}, t) = \mathcal{L}^{-1}\left\{P\left(\vec{k}, s\right)\right\}$ can be performed analytically since $P(\vec{k}, s)$ is a rational function in s (see the appendix); (iii) (6) gives us an unexpected handle to detect and quantify the intermittent behavior also from the mean square displacement $MSD(t)$, which can

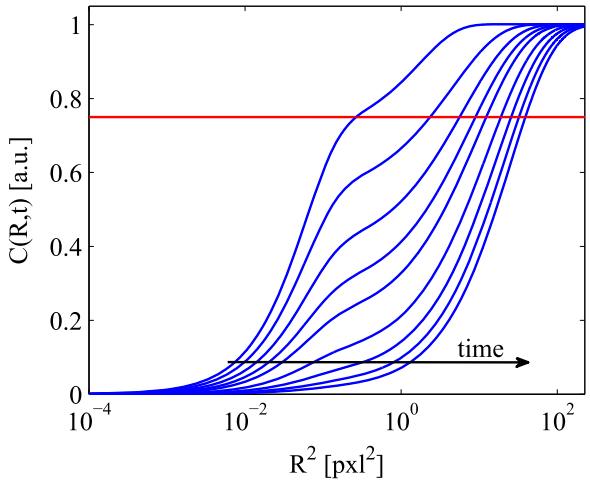

Figure 1. Cumulative distribution functions of switching between a diffusive state and a trapping state ($D_1 = D = 0.5$ pixel^2/s, $D_2 = 0$, $v_1 = v_2 = 0$, $\lambda_1/\lambda_2 = T_2/T_1 = 3$, and $\omega = 0.12$ pixel) in a 2-dimensional space. For the sake of clarity, only 9 curves at $t = 1,\ 5,\ 10,\ 15,\ 20,\ 30,\ 40,\ 50,\ 60$ s are displayed. The red solid line represents the steady-state probability $p_2^{SS} = \lambda_1/(\lambda_1 + \lambda_2) = 0.75$.

be directly calculated from $P(\vec{k}, t)$ (see the appendix), but only in the presence of at least one biased diffusion state. Even for the simplest case (i.e., $d = 1$ and $n = 2$), $MSD(t)$ not only contains a diffusion term linear in t and a transport term quadratic in t, but also athird non-linear term that dampens out on the time scale of the switching between the two states:

$$MSD(t) = 2\frac{\lambda_1 D_2 + \lambda_2 D_1}{\lambda_1 + \lambda_2}t + \left(\frac{\lambda_1 v_2}{\lambda_1 + \lambda_2}\right)^2 t^2 + \\ + \frac{2\lambda_1\lambda_2 v_2^2}{(\lambda_1 + \lambda_2)^3}\left(1 - \frac{1 - \exp\left(-(\lambda_1 + \lambda_2)t\right)}{(\lambda_1 + \lambda_2)t}\right)t \tag{8}$$

Figure 1 shows representative cumulative distribution functions (CDFs, blue solid lines) of particles that undergo intermittent mobility between a diffusive state and a trapping state ($D_1 = D = 0.5$ pixel^2/s, $D_2 = 0$, $v_1 = v_2 = 0$, $\lambda_1/\lambda_2 = T_2/T_1 = 3$, and $\omega = 0.12$ pixel). At $t = 1$ s the diffusive and trapping states are weakly coupled, and the total CDF can be well approximated by the linear combination of the diffusive and trapping CDFs with $p_1^{SS} = \lambda_2/(\lambda_1 + \lambda_2) = 0.25$ and $p_2^{SS} = \lambda_1/(\lambda_1 + \lambda_2) = 0.75$ being the respective weights. This is well indicated by the kink intercepting at $t = 1$ s the red solid line that represents the steady-state probability p_2^{SS}. As t increases, the kink disappears (i.e., the two states become more coupled) and at large times ($t \gg T_2$), the CDF is quite comparable to the one of a single diffusive state with an effective diffusion coefficient $D_{eff} = p_1^{SS} D = 0.25D$, i.e., at large times, it is likely that the particles diffuse more slowly. Interestingly, this result is also confirmed by (8) if one sets $D_2 = 0$ and $v_2 = 0$.

The occupation probability in its Fourier space $P(\vec{k}, t)$ can be directly exploited to evaluate the spatio temporal correlation function defined in the STICS master equation [21], which is proportional to the following spatial convolution:

$$C_{PP}(\vec{r}) \underset{\vec{r}}{\otimes} P_{\vec{r}_\tau|\vec{r}_0}(-\vec{r}, \tau) \tag{9}$$

where $C_{PP}(\vec{r})$ is the spatial autocorrelation of the experimental point spread function (PSF). Alternatively, it might be used for calculating the cumulative probability $C(R, t)$ necessary in the PICS analyses [22]. For this purpose, we obtained the analytical relation between $C(R, t)$ and $P(\vec{k}, t)$ (see the appendix):

$$C(R, t) = R \int_0^\infty dk\, J_1(Rk) \exp\left(-\omega^2 k^2\right) \times \left[\frac{1}{2\pi} \int_0^{2\pi} d\theta\, P(k, \theta + \pi, t)\right] \tag{10}$$

where J_1 is the Bessel function of the first kind (of order 1) and ω is the localization uncertainty of the particle.

3. Intracellular trafficking of nanoparticles in living cells

We applied the intermittent transport model to the intracellular trafficking of cationic lipid/DNA complexes in living Chinese hamster ovarian (CHO) cells. Lipid/DNA nanoparticles are a self-assembled complex of plasmid DNA and a mixture of cationic liposomes. Depending on mixing ratio and the particular lipid used, the DNA is packed within the lipid bilayers, building up a multilamellar structure, or may be coated with a lipid monolayer arranged in a hexagonal lattice [25, 26]. Several biomedical applications have exploited lipid/DNA complexes as nanoparticle-based carriers thanks to their low immunogenicity/toxicity and relative ease in synthesis and functionalization [27, 28].

In previous studies by SPT and STICS [15, 23, 24], we demonstrated that lipid/DNA nanoparticles undergo both pure diffusion and biased diffusion, no matter which lipid formulation was prepared. We found that the active transport in the cell was mainly mediated by the microtubule network.

Hence, for data interpretation, we consider here a 3-state model in which transitions between a regular diffusion state '1' ($D_1 = D$, $v_1 = 0$, switching timescale T_1) and a biased diffusion state '2' ($D_2 = D$, $v_2 = v$, switching timescale T_2) may occur. In addition, we considered a state '3' that characterizes immobile vesicles within the experimental timescale and that is uncoupled from states '1' and '2' ($D_3 = v_3 = 0$, $T_3 \gg t_{exp}$). This last fraction resembles nanoparticles that are trapped in subcellular crowded regions (e.g., the perinuclear region). The intermittent behavior of lipid/DNA nanoparticles is schematically described in figure 2.

Culture conditions for CHO cells, and lipid/DNA nanoparticle preparation and administration were carried out as described in [23]. The DNA inside the nanoparticles was Cy3-labeled plasmid DNA (λ_{exc} = 550 nm and λ_{em} = 570 nm), purchased from Mirus Bio. Samples were mounted onto an inverted widefield microscope equipped with a 100× oil objective (NA = 1.4). Cells were kept at 37 °C and 5% of CO_2 during data acquisition. Measurements were done by illumination of the sample with a 514 nm laser for 5 ms at an intensity of 0.3 kW cm^{-2}. Time series of images (200 frames @ 1 Hz) were acquired, setting a region of interest of 100 × 100 pixels (pixel size of 202 ± 2 nm) on a liquid nitrogen-cooled black-illuminated charge coupled device (CCD)-camera. The image analysis was performed following the PICS method, discussed in detail in [22]. Briefly, the x/y position of individual

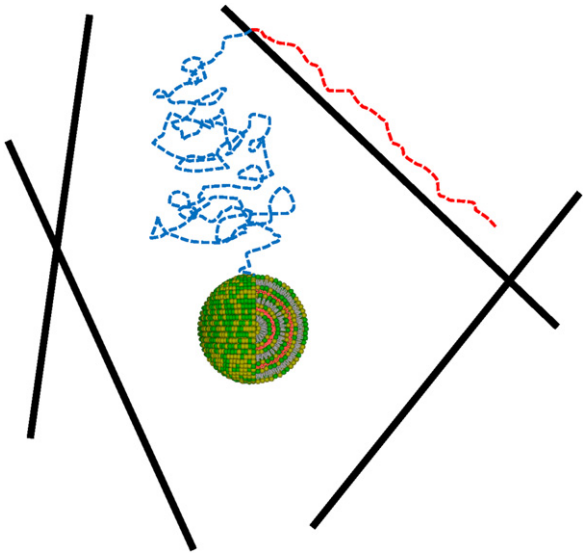

Figure 2. Schematic representation of the intermittent transport of lipid/DNA nanoparticles. The nanoparticle is sectioned to show the DNA (small red rings) packed in between the binary lipid bilayers (green and yellow spheres represent the headgroups of two distinct lipids). The dashed red line represents the trajectory along the microtubule (solid black line) in the biased diffusion state, while the dashed blue one depicts the free diffusive path inside the cytoplasm.

nanoparticles was determined frame by frame using a least-squares 2D Gaussian fit with high localization precision ($\omega_{exp} = 27 \pm 12$ nm). The super-resolved images were spatio temporally correlated analogously to what is done by STICS [19]. For every time delay t, an integration over a circular spatial domain allowed us to obtain experimental CDFs that needed to be further corrected for random correlations.

Using an unweighted non-linear least-squares method, the experimental CDFs were therefore individually fitted according to the following model:

$$C_{fit}(R,\, t) = R \int_0^{\infty} dk\, J_1(Rk) \exp\left(-\omega^2 k^2\right) \times \left[\frac{1}{2\pi} \int_0^{2\pi} d\theta (\alpha\, P(k,\, \theta + \pi,\, t) + (1 - \alpha)) \right] \tag{11}$$

where $P(k,\, \theta + \pi,\, t)$ has the form (cf (6)):

$$P(k,\, \theta + \pi,\, t) = \exp\left(-\frac{t}{2} X \right) \times \left[\cosh\left(\frac{t}{2}\sqrt{Z} \right) + \frac{Y}{(\lambda_1 + \lambda_2)\sqrt{Z}} \sinh\left(\frac{t}{2}\sqrt{Z} \right) \right]$$

$$X = \lambda_1 + \lambda_2 + 2k^2 D + ikv \cos\theta$$

$$Y = (\lambda_1 + \lambda_2)^2 - ikv(\lambda_1 - \lambda_2)\cos\theta$$

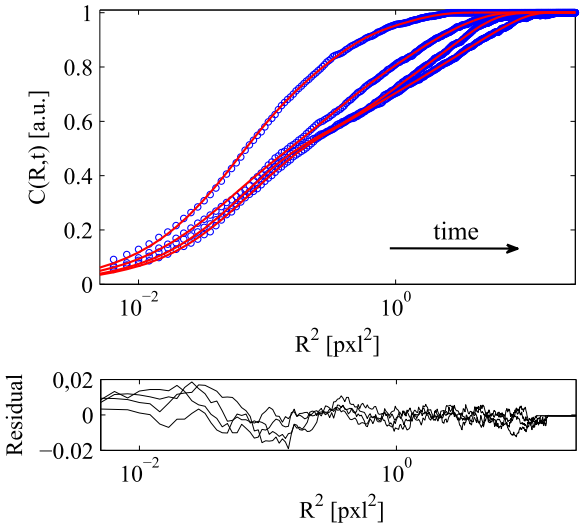

Figure 3. Experimental (blue circles) and theoretical (red lines) cumulative distribution functions. The fitting routine has been run individually for each time, up to $t = 20$ s, but for the sake of clarity, only 4 curves are displayed (i.e., at $t = 1, 5, 10, 20$ s). Residuals are also reported to support the goodness of fit (black line).

$$Z = X^2 - 4k^2D\left(k^2D + \lambda_1 + \lambda_2\right) + \\ - 4iv\left(k\lambda_1 + k^3D\right)\cos\theta \tag{12}$$

Figure 3 shows the experimental (blue circles) and fitted (red lines) cumulative distribution functions at $t = 1, 5, 10, 20$ s. It is noteworthy to observe that the kink introduced in figure 1 is here overshadowed for the presence of biased diffusion and a third independent (i.e., not switching) immobile fraction.

We were therefore able to determine the average fraction $\langle\alpha\rangle = 0.63 \pm 0.05$ of nanoparticles undergoing transitions between passive and active transport with average steady-state probabilities $\langle p_1^{SS}\rangle = \langle T_1/(T_1 + T_2)\rangle = 0.77 \pm 0.06$ and $\langle p_2^{SS}\rangle = \langle T_1/(T_1 + T_2)\rangle = 0.23 \pm 0.06$, respectively (see table 1). In addition, mean experimental values of diffusion coefficients ($\langle D\rangle = (7.6 \pm 2.0)10^{-4}\ \mu\text{m}^2\,\text{s}^{-1}$) and velocity ($\langle v\rangle = 34 \pm 6$ nm s^{-1}) corroborate our previous results by SPT and STICS [15, 23, 24].

Lastly, the fitting allowed us to estimate average values for T_1 and T_2 (i.e., $\langle T_1\rangle = 16$ s and $\langle T_2\rangle = 5$ s). The time-scales that characterize the intermittent behavior of lipid/DNA nanoparticles provide important insights into the time spent in the diffusive state, when the nanoparticles are much more likely to react and to release the DNA.

In conclusion, we presented here a robust analytical tool to investigate the intermittent transport of particles by either image correlation spectroscopy techniques or single particle tracking techniques.

Table 1. Average dynamical parameters were obtained by a parametric bootstrapping method (20 resamplings). Here we report the mean and standard deviation values calculated from the bootstrapped parameters for $t > 10$ s.

α ($a.\ u.$)	p_1^{SS} ($a.\ u.$)	D ($10^{-4}\mu m^2\ s^{-1}$)	v (nm/s)	ω (nm)
0.63 ± 0.05	0.77 ± 0.06	7.6 ± 2.0	34 ± 6	21 ± 3

Acknowledgments

SC and GC acknowledge financial support by the Ministry of Education, University and Research (Futuro in Ricerca, Grant No. RBFR08TLPO). This work is part of the research programme of the Foundation for Fundamental Research on Matter (FOM), which is part of the Netherlands Organisation for Scientific Research (NWO).

Appendix.

A.1. From $P(\vec{k}, s)$ to $P(\vec{k}, t)$

To obtain $P(\vec{k}, t)$, it is necessary to calculate the inverse Laplace transform of the following rational functions:

$$F_1(s) = \frac{\prod_{i=1}^{n-1} (s - a_i)}{\prod_{j=1}^{n} \left(s - b_j\right)} \tag{A.1}$$

$$F_2(s) = \frac{\prod_{i=1}^{n-2} (s - a_i)}{\prod_{j=1}^{n} \left(s - b_j\right)} \tag{A.2}$$

where $a_i, b_j \in \mathbb{C}$. After partial fraction decomposition, $\mathcal{L}^{-1}\left\{F_1(s)\right\}$ and $\mathcal{L}^{-1}\left\{F_2(s)\right\}$ are obtained analytically.

A.2. Mean square displacement from $P(\vec{k}, t)$

It is possible to obtain the mean square displacement (MSD) by calculating the second derivative of $P(\vec{k}, t) = \mathcal{L}^{-1}\{P(\vec{k}, s)\}$ with respect to $\vec{k}$ and subsequently setting each component of $\vec{k}$ to zero:

$$\begin{aligned} MSD(t) &= \int_{\mathbb{R}^d} d\vec{r}\ \ \vec{r}^{\,2}\, P\left(\vec{r}, t\right) \\ &= -\mathcal{L}^{-1}\left\{ \sum_{m=1}^{d} \frac{\partial^2}{\partial k_m^{\,2}} P\left(\vec{k}, s\right) \Big|_{\vec{k}=\vec{0}} \right\} \end{aligned} \tag{A.3}$$

A.3. Cumulative probability $C(R,t)$ from $P(\vec{k},t)$

From the PICS theory [22], we know that $C(R, t)$ is obtained by integrating the 2-dimensional spatial correlation function (substantially the same as the STICS master equation [21]) over a circular domain $C = \{(x, y): \sqrt{x^2 + y^2} \leqslant R\}$. Hence, we have to calculate:

$$\begin{aligned} C(R, t) &= \int_C A_{PSF}(\vec{r}) \otimes_{\vec{r}} P(-\vec{r}, t) \\ &= \int_{\mathbb{R}^2} d\vec{r}\ \ circ\left(\frac{\sqrt{x^2 + y^2}}{R}\right)\left[A_{PSF}(\vec{r}) \otimes_{\vec{r}} P(-\vec{r}, t)\right] \\ &= \mathcal{F}\left\{circ\left(\frac{\sqrt{x^2 + y^2}}{R}\right)\right\} \otimes_{\vec{\xi}=\vec{0}} \mathcal{F}\left\{A_{PSF}(\vec{r}) \otimes_{\vec{r}} P(-\vec{r}, t)\right\} \\ &= \left[RJ_1(Rk)k^{-1}\right] \otimes_{\vec{\xi}=\vec{0}} \left[\exp\left(-\omega^2 k^2\right) P(k, \theta + \pi, t)\right] \\ &= R\int_0^{\infty} dk\ J_1(Rk) \exp\left(-\omega^2 k^2\right) \\ &\quad \times \left[\frac{1}{2\pi}\int_0^{2\pi} d\theta\ P(k, \theta + \pi, t)\right] \end{aligned} \tag{A.4}$$

where J_1 is the Bessel function of the first kind (of order 1), $A_{PSF}(\vec{r})$ is the autocorrelation of the laser point spread function (PSF), and all Fourier transforms are in the non-unitary angular frequency form. Remarkably, this relation is valid only for a 2-dimensional space ($d = 2$). An integration over a spherical domain is necessary for a 3-dimensional PICS analysis. The double integration is numerically time consuming when it is necessary to call (A.4) in a non-linear least-squares fitting routine. For this reason, considering (A.4) as an Hankel transform of order 1, one can obtain the equivalent but less time-consuming expression:

$$\begin{aligned} &\exp\left(-\omega^2 k^2\right)\left[\frac{1}{2\pi}\int_0^{2\pi} d\theta\ P(k, \theta + \pi, t)\right] \\ &= 1 - k\int_0^{\infty} (1 - C(R, t))J_1(Rk)dR \end{aligned} \tag{A.5}$$

where the integral transform on the right is calculated only once before running the fitting routine.

References

[1] Bénichou O, Loverdo C, Moreau M and Voituriez R 2011 *Rev. Mod. Phys.* **83** 81
[2] Ott M, Shai Y and Haran G 2013 *The Journal of Physical Chemistry* B **117** 13308–21
[3] Bell W J *et al* 1991 *Searching Behaviour: The Behavioural Ecology of Finding Resources* (London: Chapman and Hall)
[4] Huet S, Karatekin E, Tran V S, Fanget I, Cribier S and Henry J P 2006 *Biophys. J.* **91** 3542–59
[5] Gorman J and Greene E C 2008 *Nat. Struct. Mol. Biol.* **15** 768–74
[6] Hendricks A G, Holzbaur E L and Goldman Y E 2012 *Proc. Natl. Acad. Sci.* **109** 18447–52
[7] Alberts B 2002 *Molecular Biology of the Cell, 4th edition* (New York: Garland)

[8] Sheetz M P and Spudich J A 1983 *Nature* **303** 31–5
[9] Howard J, Hudspeth A and Vale R 1989 *Nature* **342** 154–8
[10] Caspi A, Granek R and Elbaum M 2000 *Phys. Rev. Lett.* **85** 5655
[11] Caspi A, Granek R and Elbaum M 2002 *Phys. Rev.* E **66** 011916
[12] Kulkarni R P, Wu D D, Davis M E and Fraser S E 2005 *Proc. Natl. Acad. Sci.* **102** 7523
[13] Bove J, Vaillancourt B, Kroeger J, Hepler P K, Wiseman P W and Geitmann A 2008 *Plant physiology* **147** 1646–58
[14] Schumann C, Schübbe S, Cavelius C and Kraegeloh A 2012 *Journal of Biophotonics* **5** 117–27
[15] Coppola S, Pozzi D, de Sanctis S C, Digman M, Gratton E and Caracciolo G 2013 *Methods Appl. in Fluoresc.* **1** 015005
[16] Shlesinger M F and Klafter J 1989 *The Journal of Physical Chemistry* **93** 7023–6
[17] Ajdari A 1995 *EPL (Europhysics Letters)* **31** 69
[18] Salman H, Abu-Arish A, Oliel S, Loyter A, Klafter J, Granek R and Elbaum M 2005 *Biophys. J.* **89** 2134–45
[19] Hebert B, Costantino S and Wiseman P W 2005 *Biophys. J.* **88** 3601–14
[20] Kolin D L, Ronis D and Wiseman P W 2006 *Biophys. J.* **91** 3061–75
[21] Potvin-Trottier L, Chen L, Horwitz A R and Wiseman P W 2013 *New J. Phys.* **15** 085006
[22] Semrau S and Schmidt T 2007 *Biophys. J.* **92** 613–21
[23] Coppola S, Estrada L C, Digman M A, Pozzi D, Cardarelli F, Gratton E and Caracciolo G 2012 *Soft Matter* **8** 7919–27
[24] Coppola S, Cardarelli F, Pozzi D, Estrada L C, Digman M A, Gratton E, Bifone A, Marianecci C and Caracciolo G 2013 *Therapeutic Delivery* **4** 191–202
[25] Li W and Szoka F C Jr 2007 *Pharmaceutical Research* **24** 438–49
[26] Caracciolo G and Amenitsch H 2012 *Eur. Biophys. J.* **41** 815–29
[27] Mintzer M A and Simanek E E 2008 *Chemical Reviews* **109** 259–302
[28] Ditto A J, Shah P N and Yun Y H 2009 *Expert Opinion on Drug Delivery* **6** 1149–60